JOURNAL OF PROPULSION AND POWER
Vol. 16, No. 2, March–April 2000

Combustion Experiments in Hydrogen Peroxide/Polyethylene Hybrid Rocket with Catalytic Ignition

E. J. Wernimont* and S. D. Heister†
Purdue University, West Lafayette, Indiana 47907

Results from 100 tests of lab-scale hybrid rocket motors using hydrogen peroxide and polyethylene are presented herein. The bulk of the tests utilized 85% hydrogen peroxide with low-density polyethylene. A new consumable catalytic-ignition device has been developed to provide rapid, reliable ignition using stabilized hydrogen peroxide. Regression measurements indicate that at low chamber pressures (100 psi) a classic diffusion-dominated behavior is noted with mass flux exponents very near the theoretical value of 0.8. However, at higher chamber pressures tested (200 and 400 psi), radiative-dominated behavior is noted for average mass fluxes varying between 0.1 and 0.3 $lb_m/(in.^2\ s)$. Through the optimization of aft mixing length, combustion efficiencies in excess of 95% were obtained in these tests. No significant nonacoustic or acoustic instabilities were noted in these tests; chamber pressure fluctuations were less than 3.5% zero-to-peak of mean.

Nomenclature

A_t	= throat area, $in.^2$
C^*	= characteristic exhaust velocity, ft/s
D_p	= port diameter, in.
dt	= differential time, s
G	= total mass flux, $lb_m/(in.^2\ s)$
g_c	= gravitational constant, $lb_m\ ft/lb_f\ s^2$
L_f	= fuel grain length, in.
L^*	= characteristic chamber dimension, in.
M_{ccb}	= consumable catalytic bed (CCB) mass, lb_m
M_f	= fuel mass, lb_m
M_{inert}	= mass of expended inerts, lb_m
M_{ox}	= oxidizer mass, lb_m
$\dot{m}_{ox}$	= oxidizer mass flow rate, lb_m/s
n	= time level
OF	= mass oxidizer/fuel mixture ratio
P_c	= head-end chamber pressure, psia
r	= fuel regression rate, in./s
t	= time, s
ρ_f	= fuel density, $lb_m/in.^3$

Superscript and Subscripts

f	= final
i	= initial
-	= burning-time averaged quantity

Introduction

IN the past few years, interest in hybrid rockets has increased because of the potential for these devices to reduce costs and enhance safety in aerospace propulsion devices. A variety of applications, including launch vehicle boosters, upper stage, and tactical systems have been identified as areas in which hybrid propulsion concepts are of interest.

We can trace the use of the hydrogen peroxide (HP)/polyethylene (PE) propellant combination to the mid-1950s.[1–3] Whereas the early tests of Moore and Berman[1] were quite successful, interest waned (most probably because of the search for higher energy propellants during this era) and essentially no published work exists for a four-decade period beginning in the mid-1950s. Current requirements for lower cost, nontoxic propulsion systems have motivated a renewed interest in this storable propellant combination. Recent efforts have been undertaken in our group,[4–9] at the University of Surrey in the United Kingdom,[10] and the U.S. Air Force Academy.[11]

Recent system studies[4,5,12] point to potential benefits of HP-oxidized systems that include its high density, ease of handling, nontoxicity, and monopropellant characteristics. For example, both turbopump and pressurization systems can utilize decomposition energy and byproducts effectively to simplify engine power cycles and tank pressurization systems. In addition, the fact that HP hybrid systems tend to optimize at high mixture ratios provides a benefit in reducing the size of the expensive, high-pressure combustion chamber that contains the fuel grain. This benefit also decreases the sensitivity of these propellants to fuel slivering because the fuel provides a smaller fraction of the total propellant mass.

Polyethylene also represents a unique fuel choice in view that the present work focuses on the use of hydroxyl-terminated polybutadiene (HTPB) as fuel. Polyethylene was selected as the fuel because it is readily accessible and is easily machined. It was found to be much simpler than HTPB to manufacture and the data would then parallel/extend the work of Moore and Berman.[1]

For these reasons, an experimental program was initiated to quantify the combustion behavior of the HP/PE hybrid propellant combination. A unique consumable catalytic ignition system was used to provide the initiation of combustion in these studies. Factors considered in the tests described in this paper include mass flux, oxidizer/fuel (OF) mixture ratio, chamber pressure, fuel grain length (L^*), and PE formulation. The test program was formulated to maximize the amount of information available to actually design a HP/PE hybrid. All of the motors fired in this investigation are approximately 50 lb_f. Concentrated hydrogen peroxide could not purchased and had to be concentrated from 50% for the majority of the firings. Consequently, it was not feasible experimentally to study scaling effects. As a result, many different parameters were studied at a single thrust level, although none were studied in tremendous detail. Most parameters were investigated across a range of total mass port flux levels allowing determination of fuel regression rate influence.

The entire test program involved firing 11 different series of motors, with each series dedicated to examination of a specific parameter. A total of 100 firings were conducted in association with these test series, which are summarized in Table 1. Testing accomplished using a radial-flow geometry (test series C in Table 1) is reported in Ref. 13. The facility is briefly described in the following section, followed by a description of the ignition system, and experimental results.

Received 29 January 1998; revision received 25 March 1999; accepted for publication 8 April 1999.

*Graduate Research Assistant; currently Staff Engineer, General Kinetics LLC, Aliso Viejo, CA.

†Associate Professor, School of Aeronautics and Astronautics; currently Professor, School of Aeronautics and Astronautics, Grissom Hall. Associate Fellow AIAA.

Table 1 Test series summary

Series	Purpose	Number of motors	Test parameters
A	System verification	12	$\bar{P}_c \sim 100$ psia; $\bar{G}$ 0.25–0.35 $lb_m/(in.^2\text{-s})$; 85% HP Interox, high density polyethylene
B	Broader flux	12	$\bar{G}$ 0.15–0.35 $lb_m/(in.^2\text{-s})$; three at 80% HP Interox
C	Radial flow motor	20	Proof of concept; 8 ignition tests
D	Polyethylene types	11	Low density polyethylene, ultra-high molecular weight
E	Higher mass flux, P_c	8	Flight weight, low density polyethylene; proof of combustion
F	New HP vendor	5	Air liquide 85% HP
G	Increase P_c	5	$\bar{P}_c \sim 200$ psia
H	Lengthen aft combustion	4	Increase by 2, 4 in.
I	Action time study	4	Two at 6, 9 s each
J	Increase P_c	5	$\bar{P}_c \sim 400$ psia
M	Increase mass flux	10	G 0.35–1.0 $lb_m/(in.^2\text{-s})$
Y	Ignition behavior	4	Visual observations, polymethyl methacrylate fuel

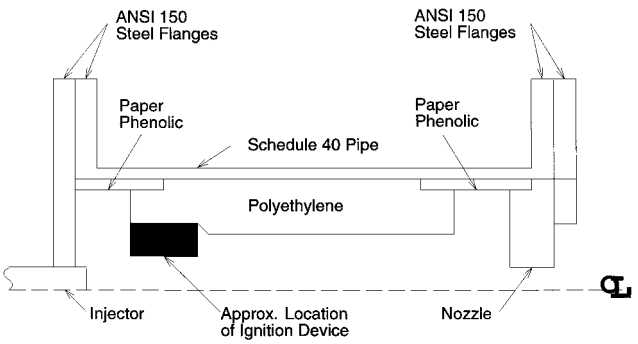

Fig. 1 Cross-sectional view of the combustion chamber.

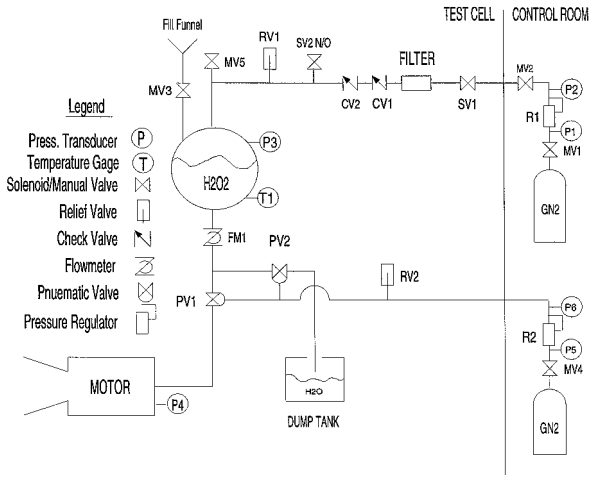

Fig. 2 Test facility schematic.

Test Apparatus/Methodology

The fluid system was designed to provide reliable combustion measurements with minimal complexity and redundant safety features. To this end, a simple cartridge-loaded combustion chamber is used with a simple "nozzle" designed to provide the required throat area without an exit cone (simple throat plug). Figure 1 highlights the 2-in.-outside diameter combustion chamber design; the catalytic ignition device is described in detail in the following section. Typical fuel grain lengths varied between 6 and 18 in. and initial port diameters varied from 0.75 to 1.25 in. The insulating materials used for these tests are paper phenolic. The nozzle material is a silica phenolic that provided a low erosion rate of less than 2.0 mil/s for the configurations fired.

A schematic of plumbing and tankage associated with the test apparatus is shown in Fig. 2. This apparatus provides for safe firing of a hydrogen peroxide hybrid rocket motor by remote operation from a concrete enclosed control room. The entire fluid system uses materials compatible with high-concentration hydrogen peroxide such as 300-series stainless steels, glass, and teflon. The high pressure HP tank is pressurized and regulated using a nitrogen "K-bottle" with manual isolation valve, MV1, depicted in Fig. 2. A second K-bottle (manual isolation valve MV4) is used to provide high pressure gas for remote actuation of stainless steel pneumatic valves denoted PV1 and PV2 in Fig. 2. During a test, the system is operated by simply opening the main oxidizer valve (PV1) until all of the HP loaded in the oxidizer tank is consumed. Gaseous nitrogen is then driven into the combustion chamber causing quenching of the remaining fuel.

As can be seen from Fig. 2, this system incorporates many safety features. Actuation of pneumatic valve PV2 provides for dumping and dilution of the HP (PV2) in the event of an emergency. Other safety features include a normally open venting solenoid valve (SV2), a remotely actuated manual vent valve (MV5), and a relief valve (RV1) on the oxidizer tank. These features were installed to allow venting of the oxidizer system in the event that undesired decomposition of the loaded HP occurs. During the entire test program, there were no occasions in which dumping of the HP was required nor did undesired decomposition occur.

Instrumentation for these tests consist of ullage and chamber pressure, oxidizer turbine flow meter information as well as axial thrust measurement. This set of information (plus pre-/posttest fuel grain measurements) is sufficient to determine motor-operating parameters as well as information on fuel regression rate. Digital data were acquired using a Pentium-based PC with a Keithley/Metrabyte analog/digital converter. This data acquisition system was used to obtain real-time display of the conditions in the oxidizer tank [temperature (T1) and pressure (P3)] during HP loading. This provided a basis to execute an emergency dumping procedure if the loaded HP began to decompose in the tank. No such events were noted in the entire test series.

During a firing, the data acquisition system is used to sample the motor operation parameters at 350 Hz per instrument. In each test, oxidizer flow rate is held approximately constant using the self-limiting combustion behavior of hybrid rocket motors, i.e., the rate of oxidizer injected into the combustion chamber is a direct function of the ullage-to-chamber pressure differential and the chamber pressure is also dependent on the oxidizer flowrate (for given nozzle and fuel port diameters). Assuming no throat erosion, both chamber pressure and oxidizer flow rate may be held constant by maintaining a constant ullage pressure. Constant ullage pressure is achieved by regulated nitrogen pressurant gas. This technique is used for all of the tests presented in this paper.

Consumable Ignition Device

One of the challenges in creating a workable hybrid propellant combination lies in the development of an ignition concept that provides a rapid and reproducible rise in chamber pressure and thrust. In the past, secondary injection of pyrophoric fluids, electric ignition sources, torches, and catalytic ignition systems have been used in hybrid rockets. With the exception of the catalytic system, all of these concepts require additional hardware and/or fluids to support ignition of the motor. For this reason, the catalytic concept

was pursued through the use of a consumable catalytic bed (CCB). Whereas catalytic devices such as silver screens and other materials treated with catalytic material have been used to decompose peroxide in the past,[14] the present concept[15] provides several advantages over these techniques:

1) The CCB concept supports operation with stabilized HP (successful 20-s sustained tests with stabilizer levels as high as 50 ppm). Most of the silver-based catalyst systems do not operate with stabilizers (primarily stannate and phosphate compounds) greater than approximately 5 ppm in the fluid because these materials would reduce the catalytic activity of the bed material. Use of stabilized fluid throughout this test program has been viewed as a safety enhancement.

2) The CCB provides an energetic ignition system with no inert parts, thereby maximizing the propellant mass fraction of the propulsion system.

3) Because the device requires no inert hardware (or other fluids/gases) it also represents a minimum cost ignition system.

The CCB is inserted into a pocket that was machined into the forward end of the fuel grain as noted schematically in Fig. 1. No special ignition sequence was used in any of the testing, the engine was literally "slam started" by opening valve PV2 (see Fig. 2), which provides maximum HP flow. As HP passes through passages in the CCB it is decomposed. If the HP is at sufficient concentration, the decomposition products are at a temperature such that auto-ignition of the PE occurs. As the HP flow continues, the CCB is consumed. If the CCB is sized properly, there will be enough energy in the combusting fuel grain to support thermal decomposition of the HP injected after CCB consumption; i.e., the device operates for only a small fraction of a firing.

Figure 3 highlights a group of typical ignition transients obtained with the use of 85% HP. This collection shows that the CCB is repeatable and produces rapid ignition transients. The peaks at approximately 30 ms represent a pressure overshoot because of increased oxidizer mass flow when the oxidizer valve is first opened. Because there is no cavitating venturi in the fluid system, the oxidizer mass

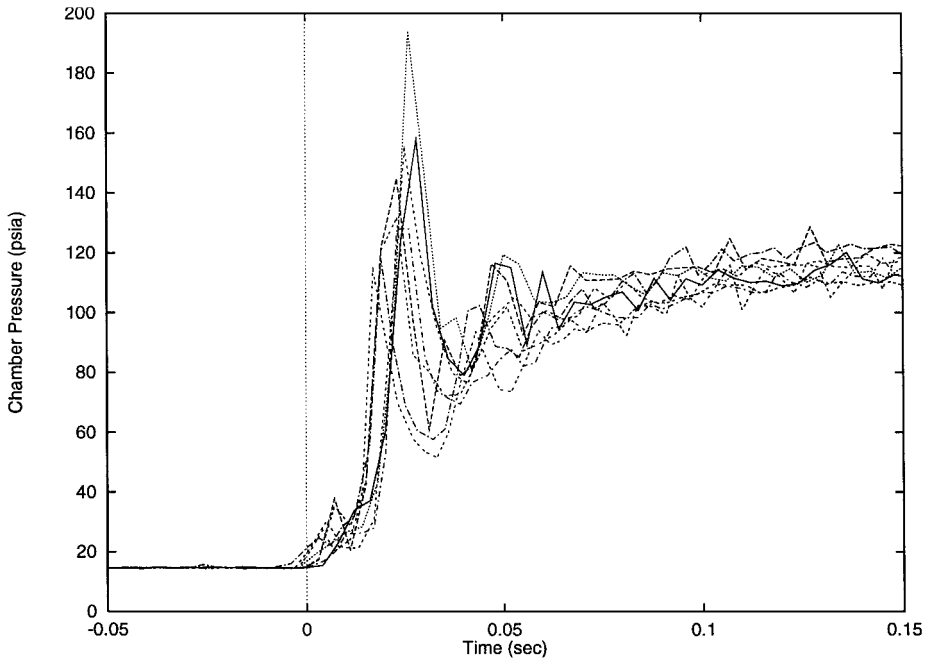

Fig. 3 Typical motor ignition traces (from D-series testing).

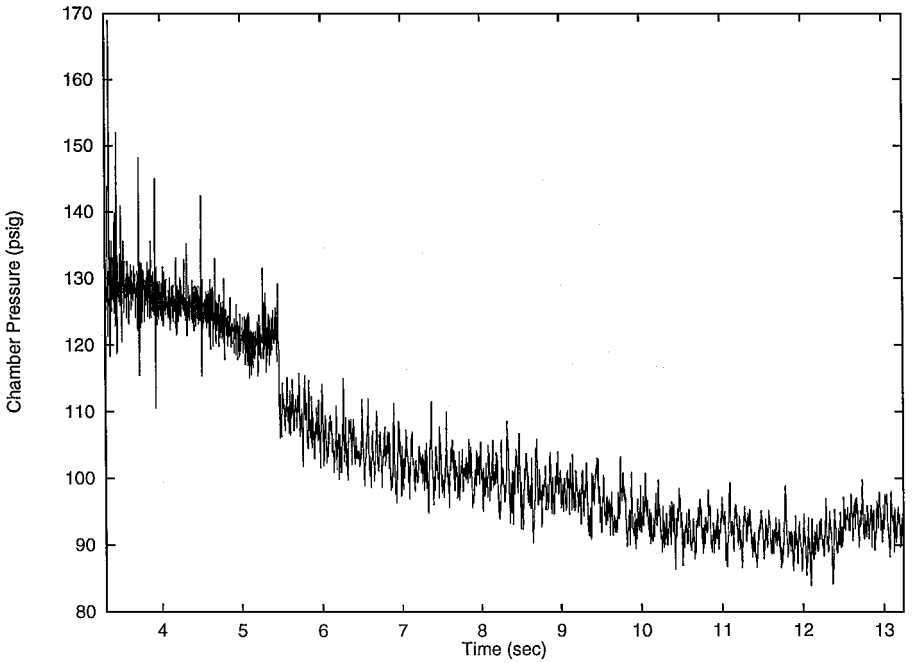

Fig. 4 Motor Y1 chamber pressure history.

flow is governed strictly by pressure differential. Consequently, initial fluid flow is greatest for the first 20 ms before the chamber pressure has a chance to climb to its steady-state value. As can be seen from Fig. 3, steady-state combustion has been achieved in 50 ms.

To aid in the understanding of the rate of consumption of the ignition device (CCB), a series of four motors (Y-series described in following section) were fired using transparent acrylic, polymethyl methacrylate (PMMA) fuel grains. A typical chamber pressure history from one of these firings (test Y1) is shown in Fig. 4. The time window in the figure captures the interval from ignition to the beginning of tailoff such that the ignition event occurs at roughly 3.3 s on this timescale. There is a noticeable decrease in chamber pressure at roughly 5.5 s (2.1 s after ignition) that is observed in most firings in our test program. This behavior was attributed to the complete combustion of the CCB. A similar behavior was noted on other PMMA firings and rapid decreases in chamber pressure were well-correlated with consumption of the CCB.

To investigate this assertion, still photographs were taken during this firing. The photos were taken with the auto-iris set on the camera so that intensity levels are not necessarily representative of flame temperature. A sequence of four photos is summarized in Fig. 5, the CCB is on the right and flow is from right to left. At ignition ($t = 3.3$ s), the fuel port is already luminous indicating reaction within the CCB. The second image, taken just prior to the chamber pressure decrease, shows complete consumption of a small portion of the CCB at one circumferential location. In the next frame available from the camera ($t = 5.5$ s) the entire aft portion of the CCB has been consumed or expelled from the motor. This event correlates well with the decrease in chamber pressure noted in Fig. 4. The final image, taken just prior to total oxidizer consumption ($t = 11.5$ s) shows a small dark region at the head-end of the grain. This dark region is where the remaining portion of the CCB is not directly reacting with hydrogen peroxide and is where thermal decomposition is probably occurring. Postfire fuel samples are in agreement with this theory; negligible regression is observed in this region.

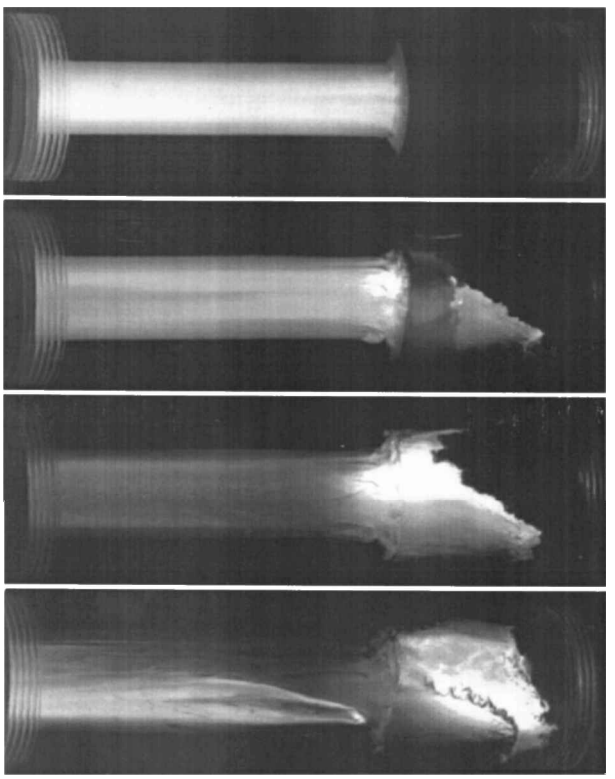

Fig. 5 Still photographs of motor Y1 showing CCB consumption. Here the CCB is located on the right-hand side of the image and flow is from right to left. From top to bottom, images are for t = 3.3, 5.45, 5.5, and 11.5 s relative to the time in Fig. 4.

One can also note an asymmetric fuel regression pattern on the last image ($t = 11.5$ s); maximum fuel regression occurs at the top of the CCB pocket in a region that was the last area to be exposed as a result of local CCB consumption. This asymmetric behavior was noted in all four PMMA firings and was attributed to nonuniformities in the spray pattern emanating from the injector.[16] The higher flow that caused local CCB consumption at $t = 5.45$ s could provide local quenching (or decreased combustion), thereby explaining the observed behavior. Whereas some asymmetries were noted in firings using PE grains, they were generally restricted to the region that housed the CCB.

Test Results

As indicated in Table 1, a broad range of tests were conducted over the 12 test series. Unfortunately, we were unable to maintain a consistent HP vendor over the three-year study. Although some differences in fluid were noted,[16] they were generally minor. Early efforts were aimed at optimizing fuel grain length so as to obtain OF ratios near the 7.5 value, which tends to maximize specific impulse for these propellants. Many of the later tests actually achieved fairly low mixture ratios (in the 5–6 range) because fuel regression rates exceeded our estimates. A complete tabulated list of all test conditions can be found in Ref. 16; we will not include all of these data here in the interest of brevity. Derivation and calculation of measurement errors for the testing present can be found in Ref. 17.

Substantial efforts were expended in quantifying combustion behavior for various PE formulations including low density PE (LDPE), high density PE, and ultra-high molecular weight materials.[16] Discussion of this area is planned for a future work; the bulk of the efforts to be described herein relate to the effects of chamber pressure, fuel grain internal diameter, fuel grain length, aft combustion length, and OF ratio on combustion performance.

Because the CCB device contributed a nonnegligible amount of mass and energy during our test burns, which typically varied between 5 and 20 s, we were forced to improve up the data reduction methodology that had typically been used by hybrid rocket experimentalists. Average regression rates and port total flux levels from a given test firing are obtained from an integral reconstruction of the entire chamber pressure history with the CCB and inerts flows taken into account. The approach begins with the determination of average characteristic velocity ($\bar{C}^*$) and oxidizer/fuel mass ratio ($\bar{OF}$) for a given test:

$$\bar{C}^* = \frac{\int_{t_i}^{t_f} P_c(t) A_t(t) g_c \, \mathrm{d}t}{M_{\mathrm{ox}} + M_f + M_{\mathrm{ccb}} + M_{\mathrm{inert}}} \tag{1}$$

and

$$\bar{OF} = \frac{M_{\mathrm{ox}}}{M_{\mathrm{fuel}} + M_{\mathrm{ccb}} + M_{\mathrm{inert}}} \tag{2}$$

The expended masses can all be measured directly with the use of pre- and postfire measurements. Instantaneous values (time level n) of total mass flux (from its definition) and fuel regression rate (assuming a steady-state balance of incoming and exiting mass flows) may then be calculated as

$$G_n(t) = \frac{\dot{m}_{\mathrm{ox}_n} + \bar{\dot{m}}_{\mathrm{ccb}_n} + r_{n-1} L_f \pi \left(2 r_{n-1} \, \mathrm{d}t + D_{p_{n-1}}\right) \rho_f}{\pi \left(2 r_{n-1} \, \mathrm{d}t + D_{p_{n-1}}\right)^2 / 4} \tag{3}$$

$$r_n(t) = \frac{P_{c_n} A_{t_n} g_c / \bar{C}^* - \dot{m}_{\mathrm{ox}_n} - \bar{\dot{m}}_{\mathrm{ccb}_n} - \bar{\dot{m}}_{\mathrm{inert}_n}}{L_f \pi \left(2 r_{n-1} \, \mathrm{d}t + D_{p_{n-1}}\right) \rho_f} \tag{4}$$

Using this process, the entire regression rate and mass flux histories may be reconstructed from the measured time-dependent data. Action time averages are computed via direct integration:

$$\bar{r} = \int_{t_i}^{t_f} r_n(t) \, \mathrm{d}t \Big/ \int_{t_i}^{t_f} \mathrm{d}t \tag{5}$$

$$\bar{G} = \int_{t_i}^{t_f} G_n(t) \, \mathrm{d}t \Big/ \int_{t_i}^{t_f} \mathrm{d}t \tag{6}$$

For the tests presented, the bias errors in regression rate and flux are estimated to be 1.9 and 1.1%, respectively. A complete description of the methodology, which will be used throughout this work, is provided in Ref. 17.

Reliable ignition and combustion was demonstrated over a range of initial oxidizer fluxes $0.1 < G_{ox} < 1.2$ $lb_m/(in.^2\ s)$ and chamber pressures $100 < P_c < 400$ psia during the testing with 85% HP. A few tests were conducted with 80% HP, but reliable ignition and combustion could not be achieved using the injector and CCB design implemented in these tests. We believe that one could design a device to operate at these lower concentrations with an improved injector (with smaller droplet sizes) and CCB designs. Our injector produced droplets that were quite large, a 350 μ volumetric mean diameter is reported by the manufacturer. Limited information[16] suggests that ignition and combustion at concentrations lower than 80% would be very difficult for PE; at these concentrations most of the decomposition energy goes into vaporizing the water in the aqueous HP. We should note that concentrations below 67% have insufficient decomposition energy to vaporize water within the mixture.

Typical chamber pressure histories obtained during the test program are shown in Fig. 6. Sharp tailoffs were always observed in the testing; action times were determined using a bisector technique[17] commonly used in solid rocket data reduction. The spike in the motor F4 and H3 traces in the interval $1 < t < 2$ s is attributed to ejection of small portions of the CCB through the nozzle. In the M1 pressure trace, a slight increase in P_c is observed after the main ignition event. This behavior is attributed to increased oxidizer flow rate because of a possible change in injector discharge coefficient.[16] Overall, the combustion obtained was very smooth as evidenced by the low amount of noise in the pressure signals. Typical unsteadiness in the pressure signals was of the order of 1–2% (zero-to-peak) of the mean pressure in this test program. This will be discussed further in the section on combustion stability behavior.

Regression Rate Behavior

Although there were test series dedicated to assessing the influence of PE polymer chemistry (chain branching and molecular weight) on fuel regression and combustion, the bulk of the measurements were obtained using LDPE fuel. A compilation of these measurements is provided in Fig. 7, which highlights dependence of regression rate on both flux level and chamber pressure. Although the low pressure (100 psi) data appear to behave a classical regression law ($r \propto G^{0.8}$) consistent with turbulent diffusion-dominated behavior,[18] the higher pressure results show a distinct insensitivity to port total mass flux (G) in the range $0.1 < G < 0.3$ $lb_m/(in.^2\ s)$. In this lower flux region, regression rates at the higher pressures tested (200 and 400 psia) are as much as 75% greater than those at low pressures. The data are consistent with a radiation-based regression law that has been theorized by Marxman.[19]

In fact, this behavior is ideal because regression rates would no longer be influenced by changes in port geometry (either shape or size). For the booster application, design studies[5] indicate an optimal mass flux level of about 0.4 $lb_m/(in.^2\ s)$ assuming a classical turbulent diffusion regression law, $r \propto G^{0.8}$. Presumably, designers could make use of this desirable behavior (flux insensitivity) for other applications as well.

To compare the data from this test program with that of previous researchers, we performed correlations assuming a classical, mass flux-dominated regression behavior. Although this approach is not warranted for the higher pressure results, it does permit gross comparisons with results of other researchers who made similar assumptions. The resulting correlations are presented in Table 2. Note that for the low pressure data the exponent of 0.78 is in close agreement with theory assuming a turbulent diffusion-dominated behavior. The exponent is reduced at the higher pressures because of the radiative-dominated behavior.

The correlations from Table 2 are compared with those obtained by other researchers in Fig. 8 plotted over the ranges of mass flux levels tested. As shown in the figure previous researchers using hydrogen peroxide[1–3,20,21] also noted deviations from turbulent diffusion dominated regression ($G^{0.8}$). Previous researchers however didn't test at low pressure (100 psia) where turbulent diffusion dominated behavior was noted in the present study. Previous research efforts with hydrogen peroxide do show a total mass flux exponential dependence similar to that explainable with radiation-driven regression. It is evident from Fig. 8 that this appears to be true independent of fuel selection and is provided only to show the

Table 2 Summary of LDPE/85% HP fuel regression flux correlations

Correlation	$\bar{P}_c$	$\bar{G}$
$0.040G^{0.78}$ ips	100 psia	0.1–0.3 $lb_m/(in.^2\text{-s})$
$0.035G^{0.52}$ ips	200 psia	0.1–0.3 $lb_m/(in.^2\text{-s})$
$0.041G^{0.49}$ ips	400 psia	0.2–0.7 $lb_m/(in.^2\text{-s})$

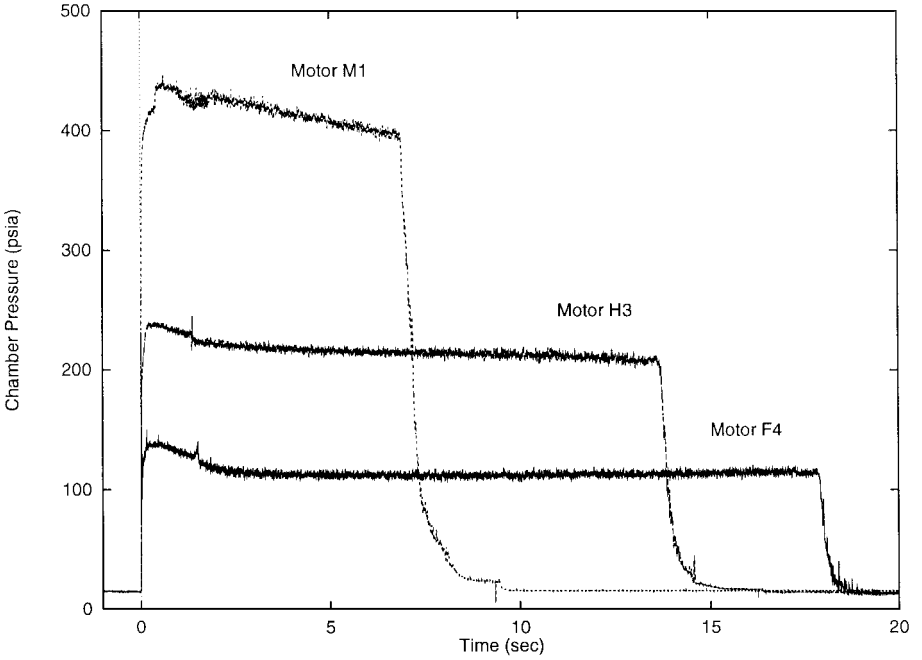

Fig. 6 Measured chamber pressure histories for motors F4, H3, and M1 at average pressures of roughly 100, 200, and 400 psi, respectively.

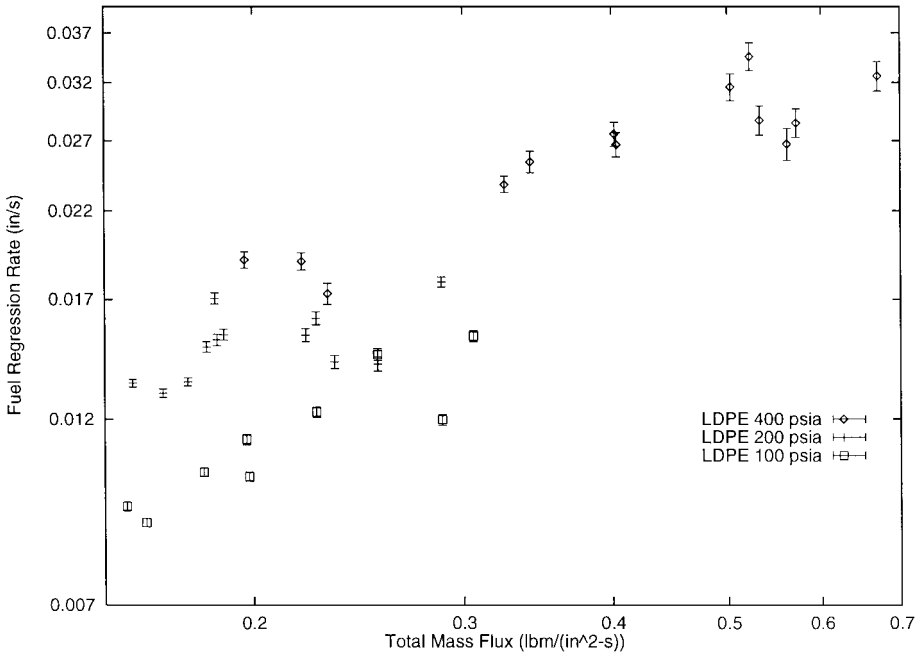

Fig. 7 LDPE fuel regression data showing effect of pressure. Values are average fuel regression rate and average total mass flux.

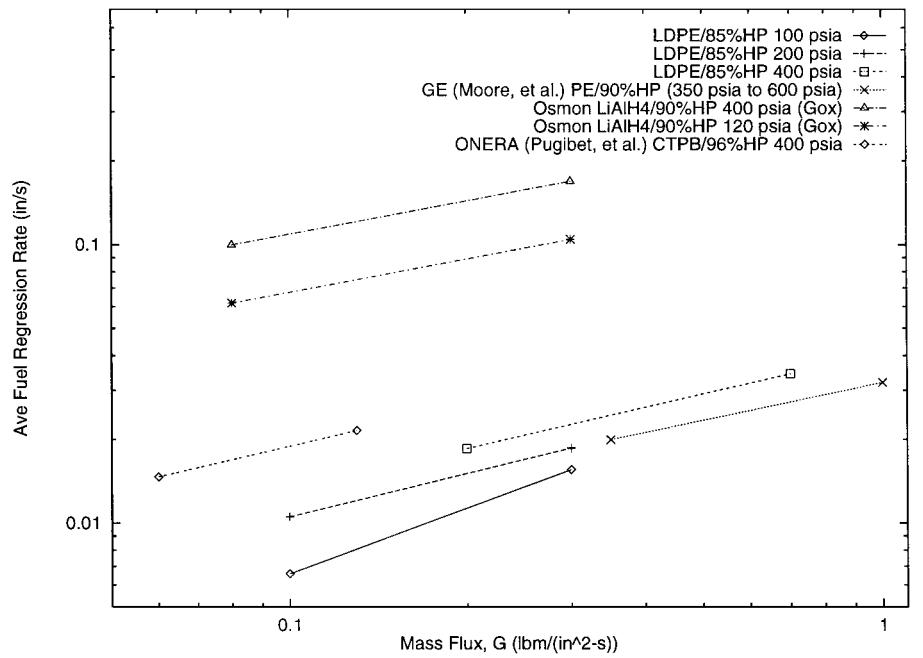

Fig. 8 Comparison of previous HP investigators regression rate measurements to present study.

trends in exponent of total mass flux. Although other researchers have also shown fuel regression for HP-oxidized systems to differ from turbulent diffusion dominated behavior, the present data are the first to show experimentally the shift to radiation-dominated behavior.

Figure 9 shows the combustion efficiency vs the characteristic chamber length L^* for the motors tested. For our purposes L^* is calculated as the combustor volume aft of the fuel grain and forward of the throat divided by the throat area. This parameter is often used in the liquids industry to design a motor for acceptable (>95%) combustion efficiency. This parameter is specific to propellant combination, but for comparison to liquid oxygen and ethyl alcohol L^* values are between 40 and 120 in (Ref. 22). Figure 9 shows that efficiency gains are derived from increased L^*, as is generally the case. Results suggest that L^* values as low as 40 in. may provide sufficient aft combustion volume for efficiencies above 90%. The calculated bias error is approximately 2.7% for the method described in Ref. 17. Please note that the authors recognize that the trend of C^* vs L^* is not necessarily correct for hybrid motors. This figure is provided for comparison to liquid rocket engines because there is no similar method established by the hybrid community.

Combustion Stability Behavior

As noted previously the sample rate for the chamber pressure was 350 Hz, which means that the Nyquist frequency is 175 Hz. The nonacoustic combustion oscillations of interest in a hybrid motor typically occur below 100 Hz (Ref. 19), hence the sample rate is sufficient to capture this phenomenon. The chamber pressure data in

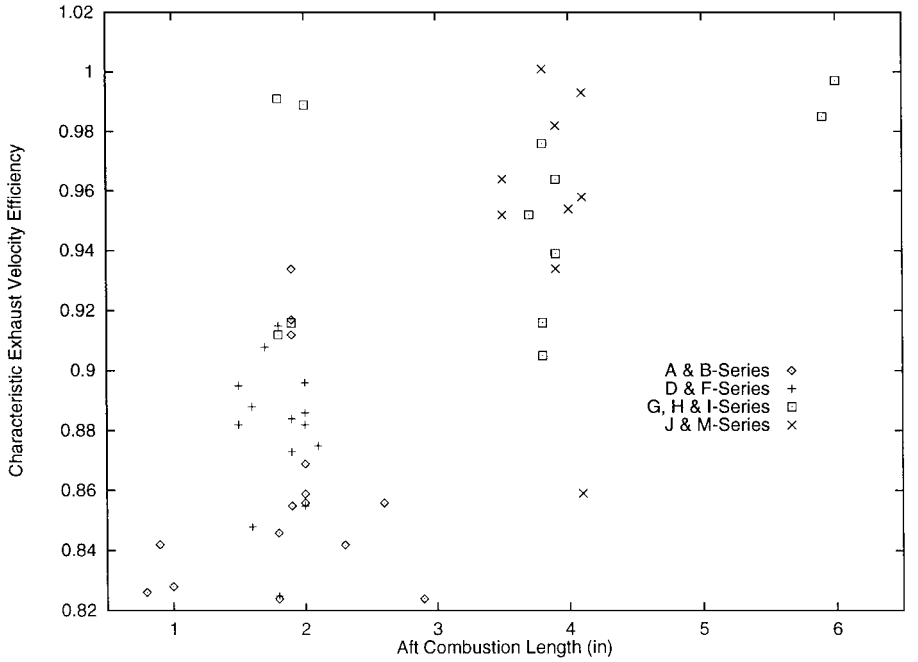

Fig. 9 Effect of aft combustion length on C^* efficiency with inerts.

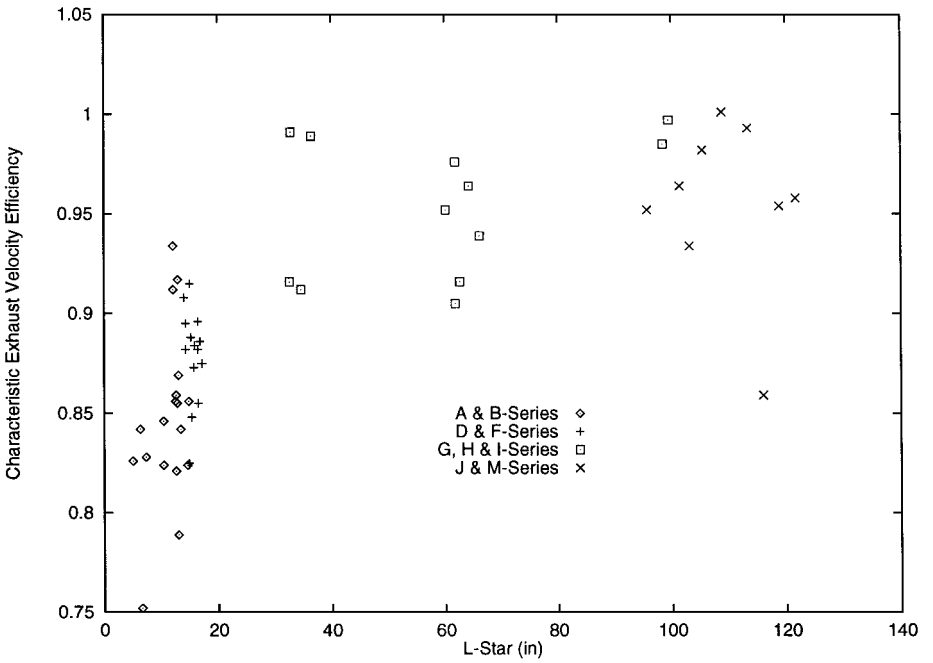

Fig. 10 Effect of L^* on C^* efficiency with inerts.

Fig. 6 show the responses for motors M1, H3, and F4. Data for motors M1 and H3 are taken with a 6-pole low-pass Butterworth filter with a theoretical cutoff frequency of 600 Hz. The low-pass filter was constructed from commercially available materials and didn't have a sharp roll off. Consequently, a cutoff frequency above the Nyquist was selected such that minimal attenuation would occur in frequencies below the Nyquist and complete attenuation would occur well below the first longitudinal mode of the motors (L1 ≈ 2 kHz). Measured behavior of the Butterworth filter showed no attenuation at 100 Hz and −30 dB at 1 kHz satisfying the desired low-pass filter behavior. Chamber pressure data from F4 shown in Fig. 6 is taken without a low-pass filter and hence the oscillations represent all waveforms (including L1, which is aliased). The oscillations associated with data taken when a low-pass filter was not used contains amplitudes no greater than 4% zero-to-peak of mean. The data where the low-pass filter was used (almost all of the chamber pressure taken in this test program used a low-pass filter) show that the amplitudes for the testing are no greater than 3.5% zero-to-peak of mean. Readers are reminded that the waveforms present are those associated with nonacoustic combustion instability and not from the L1 mode or any of its harmonics.

The data from firings where the low-pass filter Butterworth filter was used can then also be spectral-analyzed up to the Nyquist frequency (175 Hz). Figure 10 shows a typical waterfall plot from motor F4, a slight tendency for nonacoustic combustion oscillations, up to a frequency of approximately 70 Hz, is noted. Although the

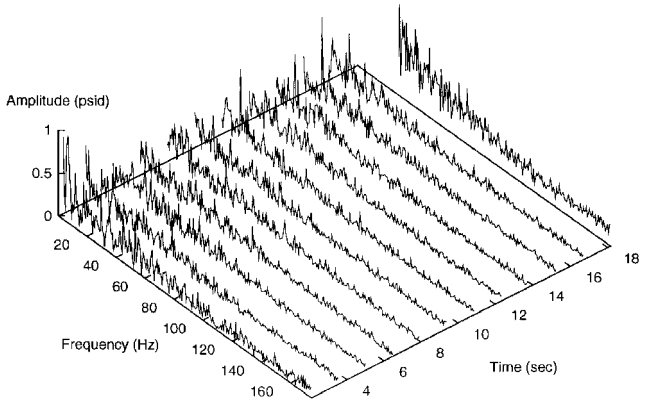

Fig. 11 Waterfall plot of chamber pressure from motor F4.

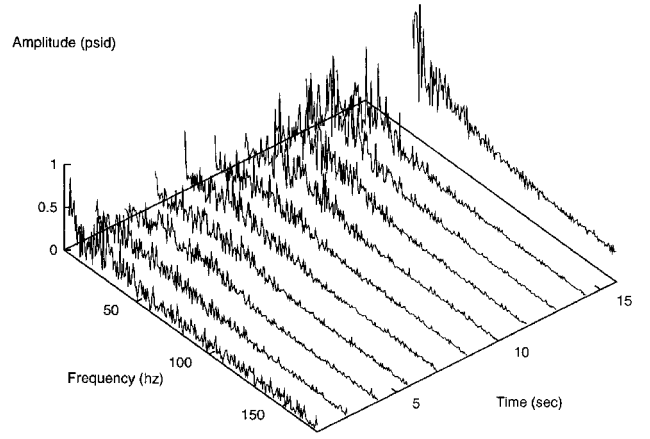

Fig. 12 Waterfall plot of chamber pressure from motor G3.

motor F4 waterfall plot in Fig. 11 shows no preferred waveform for this propellant combination, a few later motors do have preferred oscillatory waveforms. As an example, Fig. 12 shows the waterfall plot for motor G3, which has a preferred waveform at roughly 20–35 Hz with an amplitude of around 0.75 psid zero-to-peak. Three other motors (G4, I4, and M3) exhibited similar responses to that of motor G3. Other motors (J3, G5, and J5) exhibited a preferred waveform at roughly 65–80 Hz with an amplitude of around 0.5 psid zero-to-peak.

Recent theoretical efforts[23] suggest that thermal lags in the fuel can account for the low-frequency (< 100 Hz) oscillations that have been observed in numerous tests that have used either liquid or gaseous oxygen as the oxidizer. In contrast to liquid oxygen systems, which tend to optimize at *OF* values near 2.5, the HP/PE system optimizes at much higher *OF* ratio (typically around 7.5). In this case, the mass and energy addition from the fuel is much less than in oxygen-oxidized systems, thereby reducing the overall amplitude achievable. This factor may explain the lower amplitude of combustion instability for the propellant combination of HP/PE. However, we should note that all testing was performed on a fairly small scale apparatus (2-in.-diam fuel grain) and additional larger scale work will be required to confirm this hypothesis.

Conclusions

This paper summarizes combustion measurements from testing of the HP/PE hybrid rocket propellant combination. The bulk of the tests used 85% HP with LDPE, but some data are reported for other types of PE. A new CCB design has been used to provide rapid, reproducible ignition using stabilized HP. Once the CCB is consumed, the HP undergoes thermal decomposition as a result of exposure to combustion gases emanating from the ignited fuel grain. The device provides a simple, low cost (and weight) alternative for ignition of hydrogen peroxide hybrid rockets.

Measured regression rates indicate a classic turbulent diffusion-dominated behavior at chamber pressures of 100 psia, with flux exponents very near the theoretical value of 0.8. However, at higher pressures, radiation-dominated behavior in which regression appears to be insensitive to changes in flux, is noted for mass flux levels between 0.1 and 0.3 $lb_m/(in.^2\ s)$. This behavior can lead to pressure-related amplifications of regression rate as high as 75% when compared to the low pressure (100 psia) data. In theory, these conclusions should carry to larger scales because radiation effects are presumed to be scale-independent. Results are shown to be comparable to those obtained from other researchers using HP as oxidizer with various other fuels.

High combustion efficiencies (>95%) were obtained at the higher chamber pressure (200 and 400 psia) conditions by using aft mixing lengths equivalent to about two fuel grain diameters (4 in.). These lengths are consistent with L^* values (based on the chamber volume aft of the fuel grain) of about 60 in. Smooth combustion was observed in all testing, with typical chamber pressure fluctuations in the range of 1–2% (zero-to-peak) of the mean. We hypothesize that the high mixture ratio (5–8) operation of this propellant combination plays a role in reducing the amount of energy available to drive nonacoustic instabilities that the fuel (solid) contributes. Some minor activity is noted in the range of 20–80 Hz for some of the 100 motors that were tested in these efforts.

References

[1]Moore, G. E., and Berman, K., "Solid-Liquid Rocket Propellant System," *Jet Propulsion*, Vol. 26, No. 11, 1965, pp. 965–968.

[2]Moore, G. E., Driscoll, D. H., and Berman, K., "A Hybrid Rocket Propellant System: 90-Percent Hydrogen Peroxide/Solid Fuel; Part II," General Electric, TR R53A0509, Schenectady, NY, July 1954.

[3]Moore, G. E., Driscoll, D. H., and Berman, K., "A Hybrid Rocket Propellant System: 90-Percent Hydrogen Peroxide/Solid Fuel; Part I, General Considerations," General Electric, TR R52A0516, Schenectady, NY, July 1954.

[4]Ventura, M., and Heister, S. D., "Hydrogen Peroxide as an Alternative Oxidizer for a Hybrid Rocket Strap-On Booster," *Journal of Propulsion and Power*, Vol. 11, No. 3, 1995, pp. 562–565.

[5]Vonderwell, D. J., Murray, I. F., and Heister, S. D., "Optimization of Hybrid Rocket Engine Fuel Grain Design," *Journal of Spacecraft and Rockets*, Vol. 32, No. 6, 1995, pp. 964–969.

[6]Wernimont, E. J., and Meyer, S. E., "Hydrogen Peroxide Hybrid Rocket Engine Performance Investigation," *Proceedings of the AIAA/ASME/SAE/ASEE 30th Joint Propulsion Conference*, AIAA Paper 94-3147, Indianapolis, IN, June 1994.

[7]Wernimont, E. J., and Heister, S. D., "Performance Characterization of Hybrid Rockets Using Hydrogen Peroxide Oxidizer," *Proceedings of the AIAA/ASME/SAE/ASEE 31st Joint Propulsion Conference*, AIAA Paper 95-3084, San Diego, CA, July 1995.

[8]Wernimont, E. J., and Heister, S. D., "Progress in Hydrogen Peroxide Oxidized Hybrid Rocket Experiments," *Proceedings of the AIAA/ASME/SAE/ASEE 32nd Joint Propulsion Conference*, AIAA Paper 96-2696, Lake Buena Vista, FL, July 1996.

[9]Wernimont, E. J., and Heister, S. D., "Experimental Study of Chamber Pressure Effects in a Hydrogen Peroxide-Oxidized Hybrid Rocket," *Proceedings of the AIAA/ASME/SAE/ASEE 33rd Joint Propulsion Conference*, AIAA Paper 97-2801, Seattle, WA, July 1997.

[10]Sellers, J. J., "Investigations into Hybrid Rockets and Other Cost Effective Propulsion Options for Small Satellites," Ph.D. Dissertation, Univ. of Surrey, 1996.

[11]Humble, R., and Sandfry, R., "HYSTAR Hybrid Rocket Program at the United States Air Force Academy," *Proceedings of the AIAA/ASME/SAE/ASEE 33rd Joint Propulsion Conference*, AIAA Paper 97-2797, Seattle, WA, July 1997.

[12]Clapp, M. B., and Hunter, M. W., "A Single Stage to Orbit Rocket with Non-Cryogenic Propellants," *Proceedings of the AIAA/ASME/SAE/ASEE 29th Joint Propulsion Conference*, AIAA Paper 93-2285, Monterey, CA, June 1993.

[13]Caravella, J. R., Heister, S. D., and Wernimont, E. J., "Characterization of Fuel Regression in a Radial Flow Hybrid Rocket," *Journal of Propulsion and Power*, Vol. 14, No.1, 1998, pp. 51–56.

[14]Rusek, J. J., "New Decomposition Catalysts and Characterization Techniques for Rocket-Grade Hydrogen Peroxide," *Journal of Propulsion and Power*, Vol. 12, No. 3, 1996, pp. 574–579.

[15]Wernimont, E. J., Meyer, S. E., and Ventura, M. C., "A Hybrid Motor System with a Consumable Catalytic Bed, A Composition of the Catalytic

Bed and A Method of Use," U.S. Patent Application 08/623,937, Filed March 1996.

[16]Wernimont, E. J., "Experimental Study of Combustion in Hydrogen Peroxide Hybrid Rockets," Ph.D. Thesis, School of Aeronautics and Astronautics Purdue Univ., West Lafayette, IN, 1997.

[17]Wernimont, E. J., and Heister, S. D., "A Reconstruction Technique for Reducing Hybrid Rocket Combustion Test Data," *Journal of Propulsion and Power*, Vol. 15, No. 1, 1999, pp. 128–136.

[18]Marxman, G., Woolridge, C. E., and Muzzy, R. J., "Fundamentals of Hybrid Boundary Layer Combustion," *Heterogeneous Combustion*, Academic Press, New York, 1964.

[19]Marxman, G., "Boundary Layer Combustion in Propulsion," The Combustion Inst., Pittsburgh, PA, 1969.

[20]Pugibet, M., and Moutet, H., "On the Use of Hydrogen Peroxide as Oxidizer in Hybrid Systems," *La Recherche Aerospatiale*, No. 132, 1969, pp. 15–31 (Trans. by NASA as TTF-13034, May 1970).

[21]Osmon, R. V., "An Experimental Investigation of a Lithium Aluminum Hydride-Hydrogen Peroxide Hybrid Rocket," *Aerospace Chemical Engineering*, Vol. 62, No. 61, 1966, pp. 92–102.

[22]Sutton, G. P., *Rocket Propulsion Elements*, 6th Ed., Wiley, New York, 1992.

[23]Karabeyoglu, M., and Altman, D., "The Transient Behavior of Hybrid Rockets," *Proceedings of the AIAA/ASME/SAE/ASEE 33rd Joint Propulsion Conference*, AIAA Paper 97-2937, Seattle, WA, July 1997.